Geological Magazine

The Shackleton Range (East Antarctica): an alien block at the rim of Gondwana?

Nicole Krohne, Frank Lisker, Georg Kleinschmidt, Andreas Klügel, Andreas Läufer, Solveig Estrada, Cornelia Spiegel

Supplementary Material

S1. Analytical Procedures

S1.1. Thin section microscopy

Thin sections were prepared with a standard thickness of 25 µm using epoxy resin. Analysis was carried out by usage of LEICA DM EP petrographic microscope with maximum magnification of 400×.

S1.2. XRD measurement

Mineral powder (>2 µm crystallite size) was produced by hand using an opal mortar. The powder was loaded carefully into the sample holder, preventing any surface bias on the sample. Analysis was carried out at the crystallography research group of the University of Bremen. All measurement conditions valid for the machine are written in table S2.

S1.3. ICP-MS and XRF analysis

For X-ray fluorescence (XRF) analysis of major and some trace elements of sample SH08, about 0.6 g of sample powder and 3.6 g lithium tetraborate were mixed and fused beads produced. Analysis was carried out at University of Hamburg / Mineralogisch-Petrographisches Institut, using a Panalytical PW 2540. Most trace element contents were determined by inductively coupled plasma-mass spectrometry (ICP-MS) using a Thermo Element2 at University of Bremen / Department of Geosciences. About 50 mg of sample powder were digested in an ultrapure-grade HF-aqua regia mixture using an Evapoclean™ system with Savillex™ beakers. The analyte solution was spiked with 2.5 ng/ml indium as internal standard and contained 40 mg/l of total dissolved solid. In order to avoid mass interferences, the middle through heavy REE and Hf were measured at high resolution (10,000), the transition metals at medium (4,000) and all other elements at low (300) resolution.

S1.4. ^{40}Ar–^{39}Ar analysis

Samples for ^{39}Ar–^{40}Ar measurement were prepared and measured by Dr. Y. Kapusta, Actlabs, Canada. Prior irradiation in the nuclear reactor the samples were wrapped in Al-foil and loaded in alumina vial with MCA-11 flux monitors. The Ar isotope composition was measured in a Noblesse Noble Gas static mass spectrometer (NU Instrument Ltd.). The 1300ºC blank of ^{40}Ar did not exceed n*10-11 cc STP.

S1.5. Thermochronology

S1.5.1. Mineral separation

Common lab pre-processing procedures for achieving apatite separates includes rock-crushing and sorting methods (Jaw Breaker, Wilfey Table), heavy liquid (LST fastflot and Diiodmethane (CH_2I_2) and magnetic separation (Frantz Magnetscheider). Optional hand picking of apatites was conducted to enhance final purity.

S1.5.2. Fission Track analysis

AFT analysis was carried out using the external detector method following the procedures described by (Gleadow, 1984; Donelick *et al.*, 2005) and by using the zeta calibration approach (Hurford & Green, 1982); (Hurford & Green, 1983) with dosimeter glasses IRMM 540 (De Corte *et al.*, 1998). Zeta calibration was carried out on six Durango and Fish Canyon samples. Track length and D_{par} measurements followed the recommendations of Laslett *et al.* (1982); Donelick (1993); and Donelick *et al.* (2005). User length- and D_{par} calibration was applied on four samples with known track length distribution (annealed, mixed and induced lengths).

New samples were mounted in Petropoxy 154, polished and etched in 5 mol/l HNO_3 at 20°C for 20 seconds. Already mounted samples were prepared in the 1990ies and were etched in 1.13 mol/l HNO_3 for 60s at ambient room temperatures. D_{par} measurements of the already mounted samples were calibrated after recommendations of Sobel & Seward (2010) with a calibration factor of 0.14 and by direct D_{par} comparison of four samples treated with both etching conditions.

Thermal neutron irradiations were carried out in the reactor facility of FRM II (Garching, Germany) with a nominal neutron flux of 1×10^{16} n/cm^2 for all samples except for W68, W72 and W294 where a neutron flux of 1.2×10^{16} n/cm^2 was applied. Analysis was carried out with Zeiss Axioplan microscope using 1250× magnification, dry air objectives and the FT stage program of Dumitru (1993).

S1.5.3. (U-Th-Sm)/He analysis

Selection of suitable apatite crystals followed recommendations after Farley (2002). This implies >60 µm, inclusion and crack free euhedral crystals, wrapped into pre-cleaned Pt capsules. Selection was ensued at an Olympus SZX6 microscope (max. magnification of 143.75×) via transmitted and polarized light. Crystal dimensions were measured by application of the Cell A programme (Version 3.1; Olympus soft imaging solutions GmbH).

Measurement of ^{4}He, ^{235}U, ^{232}Th and ^{148}Sm was conducted at the department of sedimentology and environmental geology of Göttingen, following their laboratory procedures (http://www.sediment.uni-goettingen.de/thermochron/index.html).

S2. Tables and Figures

Table S1: Sample sites and lithologies

Sample Name	Lon	Lat	Elev. [m]	Lithology
SH 02	-80.4267	-21.7667	1065	Meta Turbidite
SH 03	-80.4217	-21.5333	1110	Meta Turbidite
SH 05	-80.5450	-20.7667	1305	Gneiss
SH 06	-80.5367	-20.5500	1255	Gneiss
SH 07	-80.6099	-20.8811	1470	Gneiss
SH 08	-80.5183	-19.0117	1355	Rhyolitc tuff
SH 09	-80.5450	-19.6033	1335	Gneiss
SH 10	-80.6396	-20.6249	1475	Gneiss
SH 11	-80.3705	-21.9687	915	Gneiss
SH 13	-80.4550	-22.2667	1105	Meta Turbidite
SH 15	-80.3467	-24.0388	1025	Gneiss
SH 16	-80.1183	-25.6333	540	Gneiss
SH 17	-80.1233	-25.7333	720	Gneiss
SH 19	-80.2567	-25.2500	890	Gneiss
SH 21	-80.3183	-24.9832	1065	Gneiss
SH 22	-80.3483	-25.0167	1010	Gneiss
SH 23	-80.3733	-25.1000	1340	Gneiss
SH 24	-80.6967	-22.6833	1515	Meta Turbidite
SH 25	-80.7333	-23.5667	1375	Meta Turbidite
W18e	-80.7157	-24.9425	1350	Pegmatite
W53	-80.7389	-25.0009	1100	Gneiss
W68	-80.7292	-25.0029	1220	Gneiss
W72	-80.6952	-24.5920	1250	Metadiorite
W181	-80.7406	-25.5275	1210	Granite
W294	-80.3860	-30.0130	570	Gneiss

Table S2: XRD measurement conditions

Measurement Conditions:	
Comment	Configuration=Sample Spinner. Owner=User-1. Creation date=08.11.2002 10:25:05 Goniometer=PW3050/60 (Theta/2Theta); Minimum step size 2Theta:0.001; Minimum step size Omega:0.001 Sample stage=Spinner PW3064 Diffractometer system=XPERT-PRO Measurement program=C:\PANalytical\Data
scan-axis	Gonio
starting position [°2Th.]	3
end position [°2Th.]	85
step width [°2Th.]	0.017
step time [s]	100
scan Modus	Continuous
OED mode	Scanning
OED legnth [°2Th.]	2.12
offset [°2Th.]	0
divergence slot [°]	fixed
divergence slot [°]	0.2177
sample length [mm]	10
measurement temperature [°C]	25
anode material	Cu
generator settings	45 kV. 40 mA
Goniometer radius [mm]	240
primary beam-monochromator	no
sample rotation	yes

Table S3: XRD reflex list

Pos. [°2Th.]	Height [cts]	FWHM [°2Th.]	d-value [Å]	Rel. int.[%]
6.21	475.9	0.1338	14.2329	0.59
10.4815	898.99	0.0836	8.44022	1.12
11.6489	843.46	0.0836	7.59689	1.05
12.4855	1039.63	0.1338	7.08967	1.29
13.3239	383.02	0.1004	6.64539	0.48
13.6288	885.22	0.1171	6.49738	1.1
13.8826	1867.37	0.0669	6.37916	2.32
15.0341	559.47	0.1673	5.89307	0.69
15.8782	296.95	0.1004	5.58163	0.37
18.0002	273.95	0.1338	4.92812	0.34
18.8368	406.29	0.1506	4.71109	0.5
19.8523	203.82	0.1004	4.47235	0.25
20.8748	19942.94	0.0836	4.25552	24.76
22.0606	5843.9	0.1004	4.0294	7.25
22.5191	1151.65	0.0836	3.94839	1.43
23.0745	1482.04	0.1004	3.85459	1.84
23.5656	6936.78	0.1171	3.77537	8.61
24.1893	3136.45	0.102	3.67637	3.89
24.2944	3774.65	0.0836	3.66373	4.69
24.5928	704.84	0.0836	3.61994	0.87
25.107	993.73	0.1338	3.54697	1.23
25.4123	1359.86	0.0669	3.50504	1.69
25.6942	3202.93	0.1673	3.46723	3.98
26.6512	80553.45	0.0669	3.34485	100
26.8573	5243.43	0.0669	3.31965	6.51
27.1129	3837.12	0.1171	3.28893	4.76
27.5707	6490.1	0.184	3.23535	8.06
27.7397	6742.54	0.0502	3.21603	8.37
27.9396	15332.14	0.1171	3.19347	19.03
28.1622	3535.33	0.0816	3.16611	4.39
28.2981	2467.51	0.1004	3.15383	3.06
29.1329	962.52	0.0502	3.06532	1.19

Table S3 (continued)

Pos. [°2Th.]	Height [cts]	FWHM [°2Th.]	d-value [Å]	Rel. int.[%]
29.3909	846.55	0.0836	3.039	1.05
29.808	7406.1	0.1338	2.99742	9.19
30.1186	3188.93	0.1338	2.96722	3.96
30.4924	2456.55	0.1171	2.93168	3.05
30.8434	2448.02	0.1673	2.89912	3.04
31.2621	1023.88	0.0836	2.86124	1.27
31.8736	368.68	0.1338	2.80773	0.46
32.3186	1002.36	0.0836	2.77008	1.24
32.9409	347.89	0.1338	2.71915	0.43
33.9531	675.63	0.1004	2.64038	0.84
34.3726	1310.3	0.1171	2.60911	1.63
34.8654	1992.48	0.1338	2.57335	2.47
35.0729	1945.53	0.0669	2.55859	2.42
35.4066	2228.05	0.102	2.53315	2.77
35.5076	2293.14	0.0669	2.52826	2.85
36.5554	5972.08	0.0612	2.45613	7.41
36.663	3291.91	0.0408	2.45525	4.09
37.3906	493.19	0.1224	2.40316	0.61
37.6644	622.34	0.2448	2.38632	0.77
38.8439	1058.19	0.0816	2.31653	1.31
39.476	4630.01	0.0816	2.28088	5.75
39.5861	2328.4	0.0408	2.28044	2.89
40.2996	2636.84	0.0612	2.23615	3.27
40.4123	1415.55	0.0612	2.23572	1.76
40.9156	246.88	0.1632	2.2039	0.31
41.2529	272.09	0.1632	2.18665	0.34
41.6541	832.01	0.2856	2.16651	1.03
42.4657	5422.02	0.0816	2.12696	6.73
42.5834	2826.59	0.0408	2.12663	3.51
42.7882	811.94	0.1632	2.11167	1.01
43.6136	359.36	0.2448	2.07361	0.45

Table S3 (continued)

Pos. [°2Th.]	Height [cts]	FWHM [°2Th.]	d-value [Å]	Rel. int.[%]
44.2011	394.52	0.204	2.0474	0.49
44.9549	914.02	0.102	2.0148	1.13
45.8043	2912.78	0.0612	1.97939	3.62
45.93	1951.15	0.0612	1.97918	2.42
47.1263	493.66	0.2856	1.92691	0.61
48.2006	864.61	0.0816	1.88644	1.07
49.2292	706.04	0.1224	1.8494	0.88
50.1493	9085.3	0.0816	1.81761	11.28
50.288	4418.25	0.0612	1.81742	5.48
50.6363	1524.99	0.102	1.80126	1.89
50.7641	1591.27	0.102	1.80149	1.98
51.1638	1265.98	0.102	1.78392	1.57
51.3106	772.67	0.0612	1.78358	0.96
52.2225	327.64	0.4896	1.75022	0.41
52.5693	285.23	0.1224	1.73949	0.35
53.2064	543.25	0.2856	1.72015	0.67
54.8858	2716.69	0.0816	1.67142	3.37
55.0311	1468.08	0.0612	1.6715	1.82
55.335	1138.8	0.0816	1.65891	1.41
55.487	596.74	0.0612	1.65884	0.74
56.5354	732.21	0.2448	1.6265	0.91
57.223	141.36	0.1224	1.60858	0.18
57.953	181.09	0.3264	1.59005	0.22
58.7049	469.86	0.204	1.57146	0.58
59.9666	6707.53	0.0816	1.54138	8.33
60.1315	3505.95	0.0612	1.54136	4.35
61.4823	496.25	0.1224	1.50696	0.62
61.9711	493	0.408	1.49624	0.61
63.5869	338.36	0.3264	1.46206	0.42
64.0467	1341.85	0.0612	1.45267	1.67
64.2236	784.28	0.0816	1.44909	0.97

Table S3 (continued)

Pos. [°2Th.]	Height [cts]	FWHM [°2Th.]	d-value [Å]	Rel. int.[%]
65.1505	680.62	0.204	1.4307	0.84
65.7947	506.29	0.0612	1.41824	0.63
66.1681	404.27	0.4896	1.41114	0.5
67.1201	280.18	0.3264	1.39342	0.35
67.7516	3895.44	0.102	1.38196	4.84
67.9454	2187.1	0.0816	1.38192	2.72
68.1505	4218.5	0.0816	1.37484	5.24
68.3332	4999.33	0.102	1.37161	6.21
68.5193	1670.12	0.0816	1.37174	2.07
69.4692	393.41	0.1224	1.35193	0.49
70.9288	360.52	0.1224	1.32765	0.45
71.9924	200.36	0.816	1.31063	0.25
73.473	1426.93	0.0816	1.28783	1.77
73.6814	875.54	0.102	1.2847	1.09
74.0577	434.25	0.3264	1.27911	0.54
74.8561	337.94	0.2448	1.26743	0.42
75.6666	1997.32	0.102	1.25586	2.48
75.8839	1128.04	0.0816	1.25591	1.4
77.6798	911.07	0.0816	1.22826	1.13
77.9011	543.31	0.102	1.22837	0.67
79.8856	1491.47	0.0816	1.1998	1.85
80.1327	881.75	0.1632	1.19672	1.09
81.1775	1098.56	0.102	1.18394	1.36
81.491	1652.66	0.1428	1.18017	2.05
81.7369	842.32	0.102	1.18017	1.05
83.8305	857.69	0.102	1.15309	1.06
84.1003	432.82	0.0816	1.15293	0.54

Figure S1

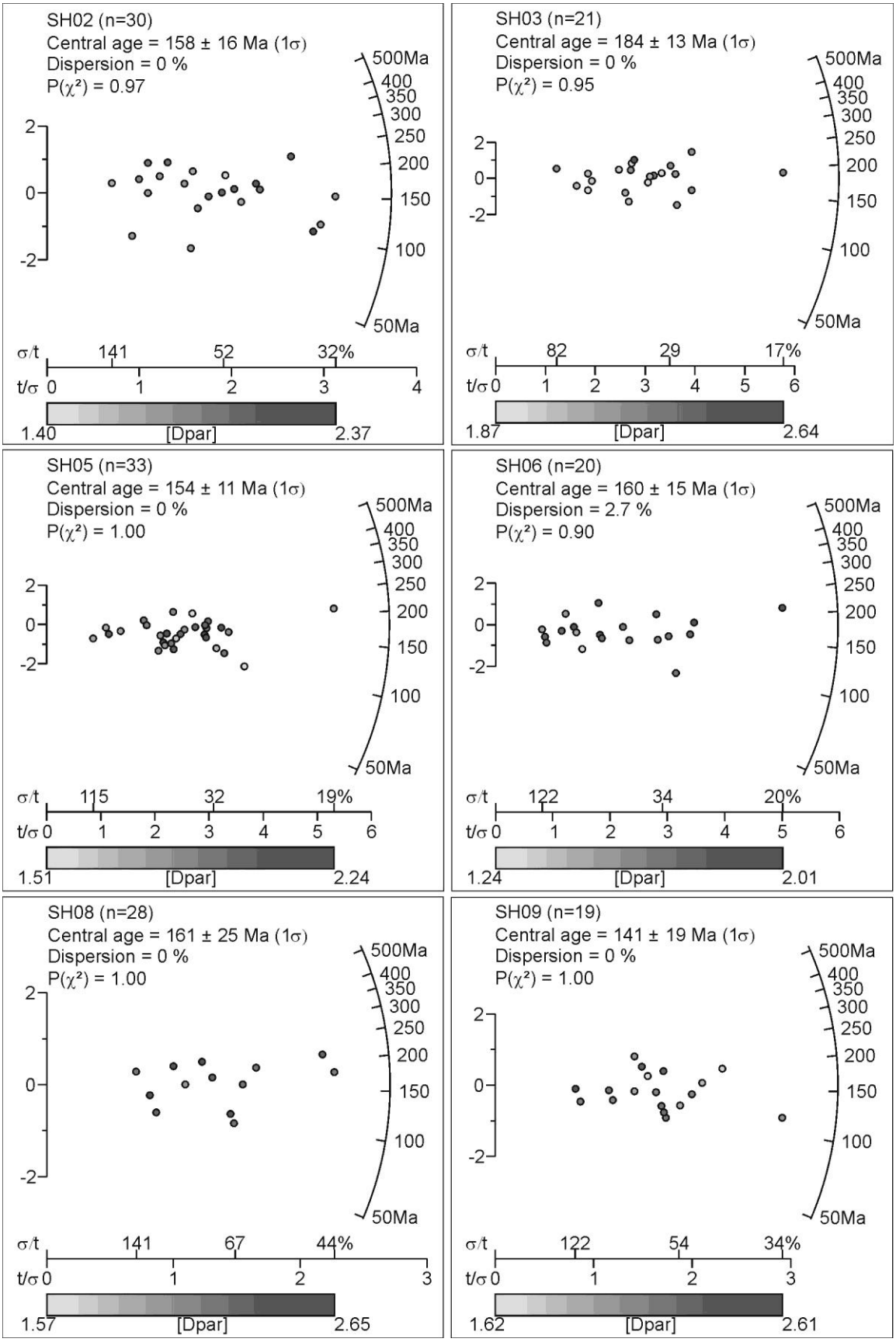
SH02 (n=30)
Central age = 158 ± 16 Ma (1σ)
Dispersion = 0 %
P(χ²) = 0.97
σ/t 141 52 32%
t/σ 0 1 2 3 4
1.40 [Dpar] 2.37
SH03 (n=21)
Central age = 184 ± 13 Ma (1σ)
Dispersion = 0 %
P(χ²) = 0.95
σ/t 82 29 17%
t/σ 0 1 2 3 4 5 6
1.87 [Dpar] 2.64
SH05 (n=33)
Central age = 154 ± 11 Ma (1σ)
Dispersion = 0 %
P(χ²) = 1.00
σ/t 115 32 19%
t/σ 0 1 2 3 4 5 6
1.51 [Dpar] 2.24
SH06 (n=20)
Central age = 160 ± 15 Ma (1σ)
Dispersion = 2.7 %
P(χ²) = 0.90
σ/t 122 34 20%
t/σ 0 1 2 3 4 5 6
1.24 [Dpar] 2.01
SH08 (n=28)
Central age = 161 ± 25 Ma (1σ)
Dispersion = 0 %
P(χ²) = 1.00
σ/t 141 67 44%
t/σ 0 1 2 3
1.57 [Dpar] 2.65
SH09 (n=19)
Central age = 141 ± 19 Ma (1σ)
Dispersion = 0 %
P(χ²) = 1.00
σ/t 122 54 34%
t/σ 0 1 2 3
1.62 [Dpar] 2.61
500Ma 400 350 300 250 200 150 100 50Ma

Figure S1 (continued)

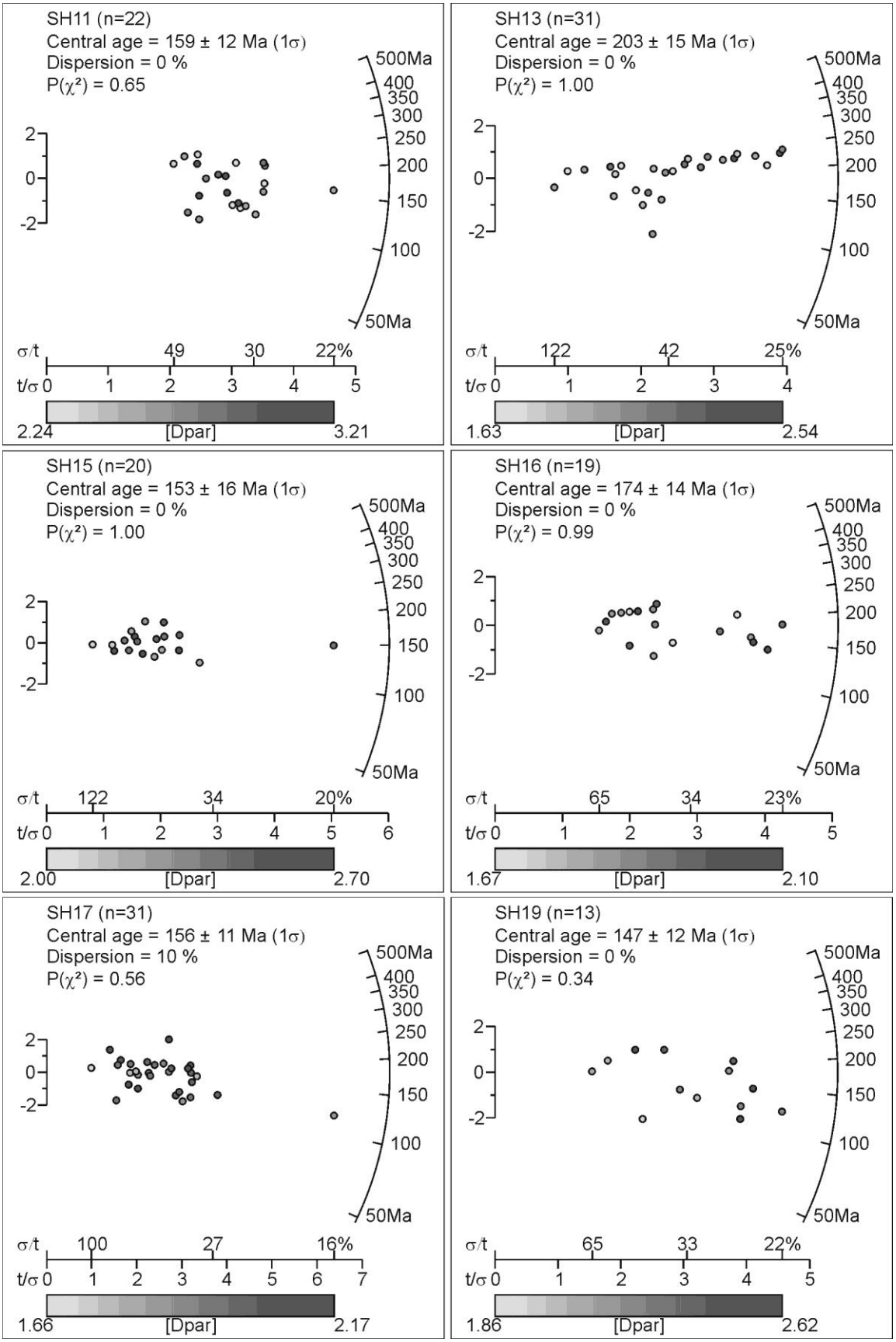

Figure S1 (continued)

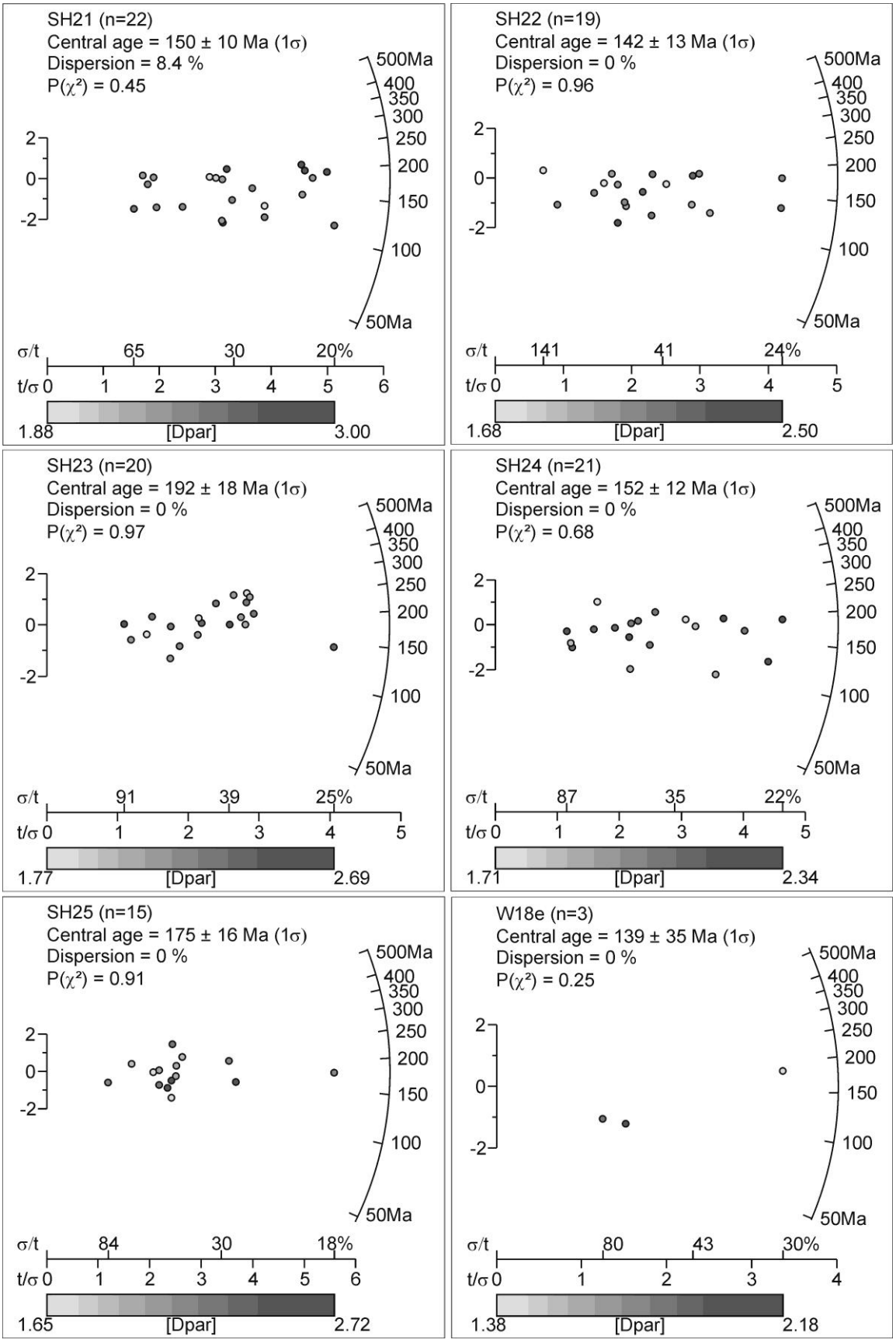

Figure S1 (continued)

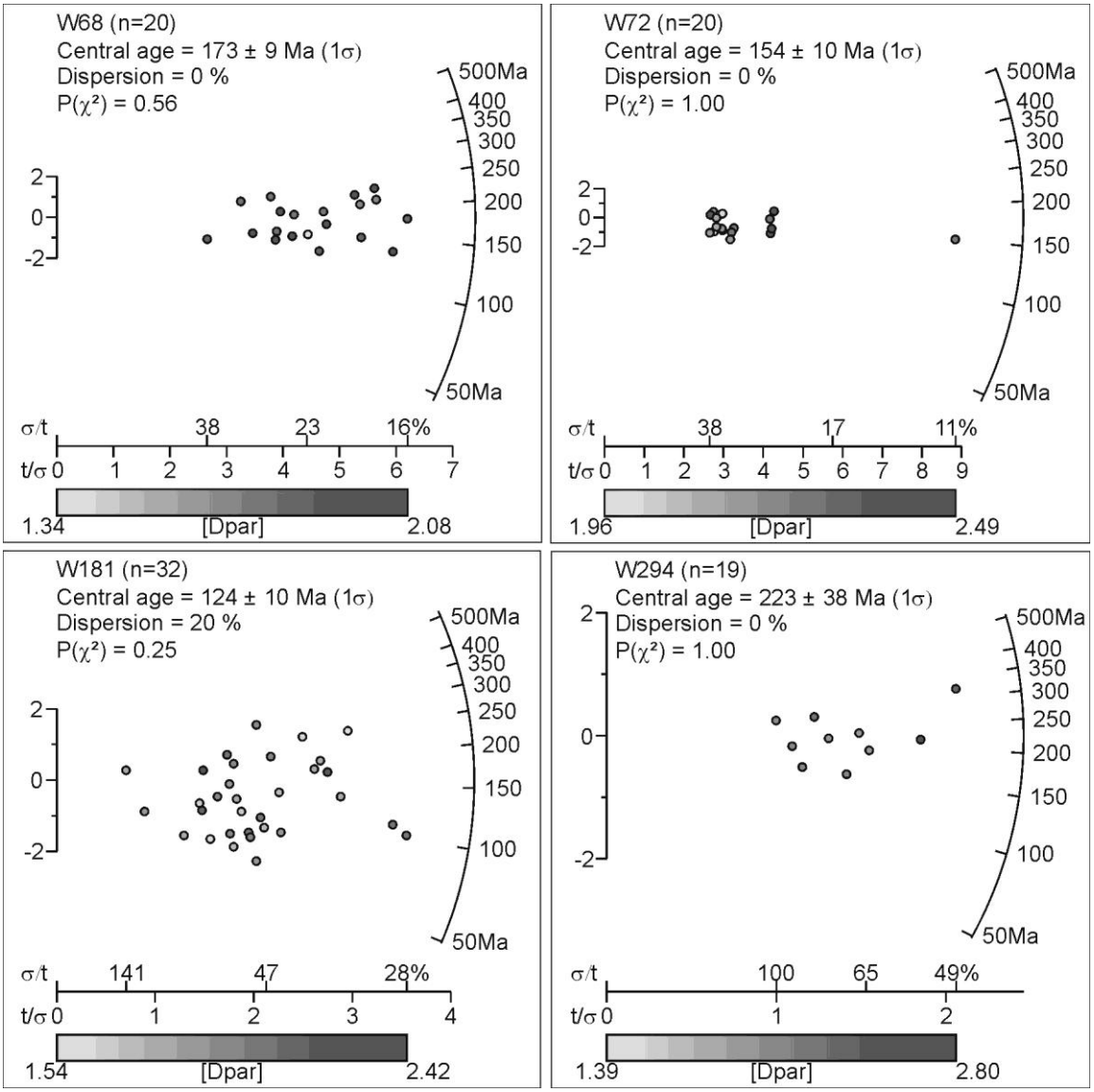

Figure S1: Radial plots of the fission track samples. Plots were created using Radial plotter (Vermeesch, 2009). Single ages are coloured reflecting their individual D_{par} value.

Figure S2

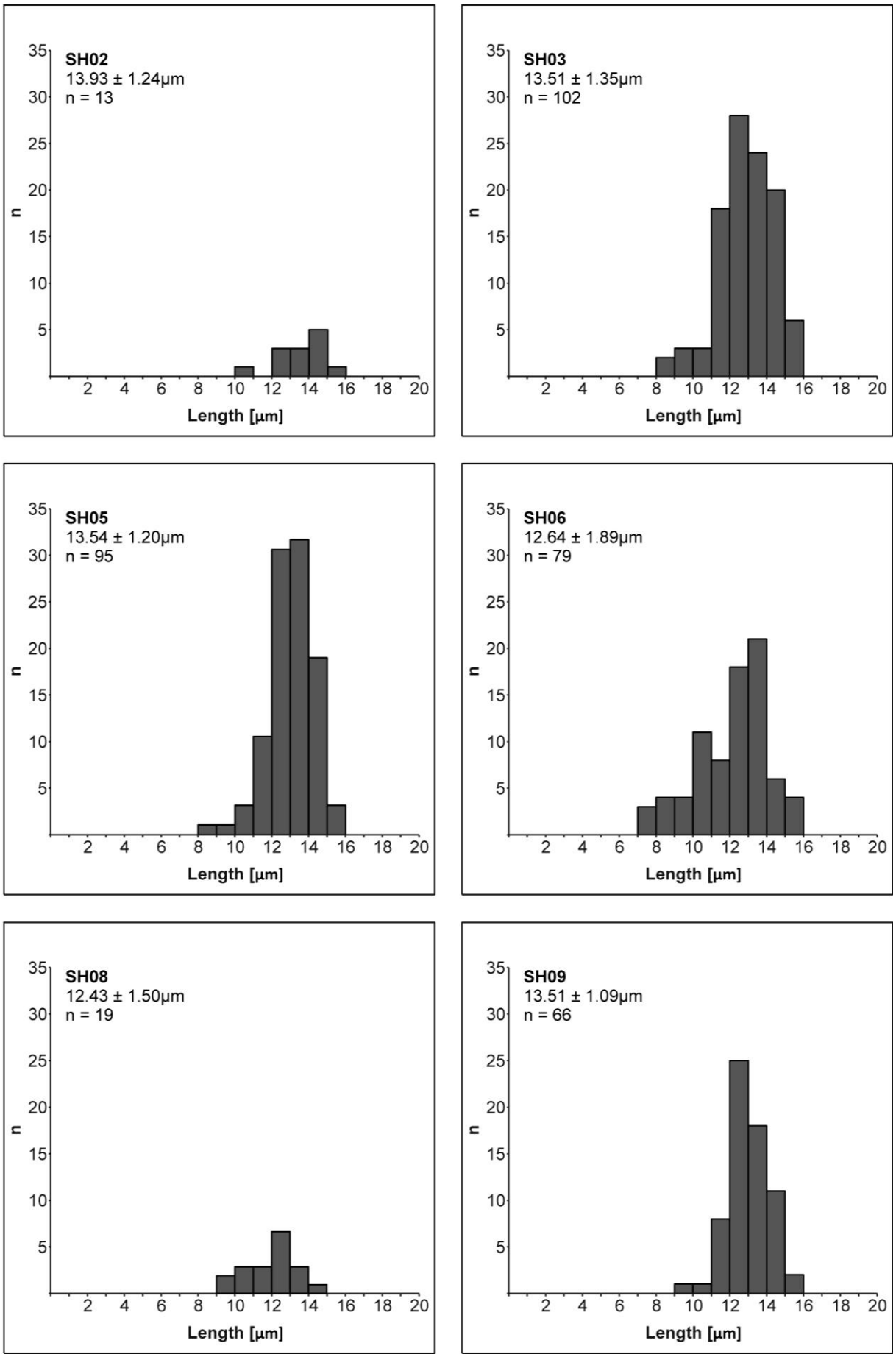
SH02
13.93 ± 1.24µm
n = 13
SH03
13.51 ± 1.35µm
n = 102
SH05
13.54 ± 1.20µm
n = 95
SH06
12.64 ± 1.89µm
n = 79
SH08
12.43 ± 1.50µm
n = 19
SH09
13.51 ± 1.09µm
n = 66
n
Length [µm]

Figure S2 (continued)

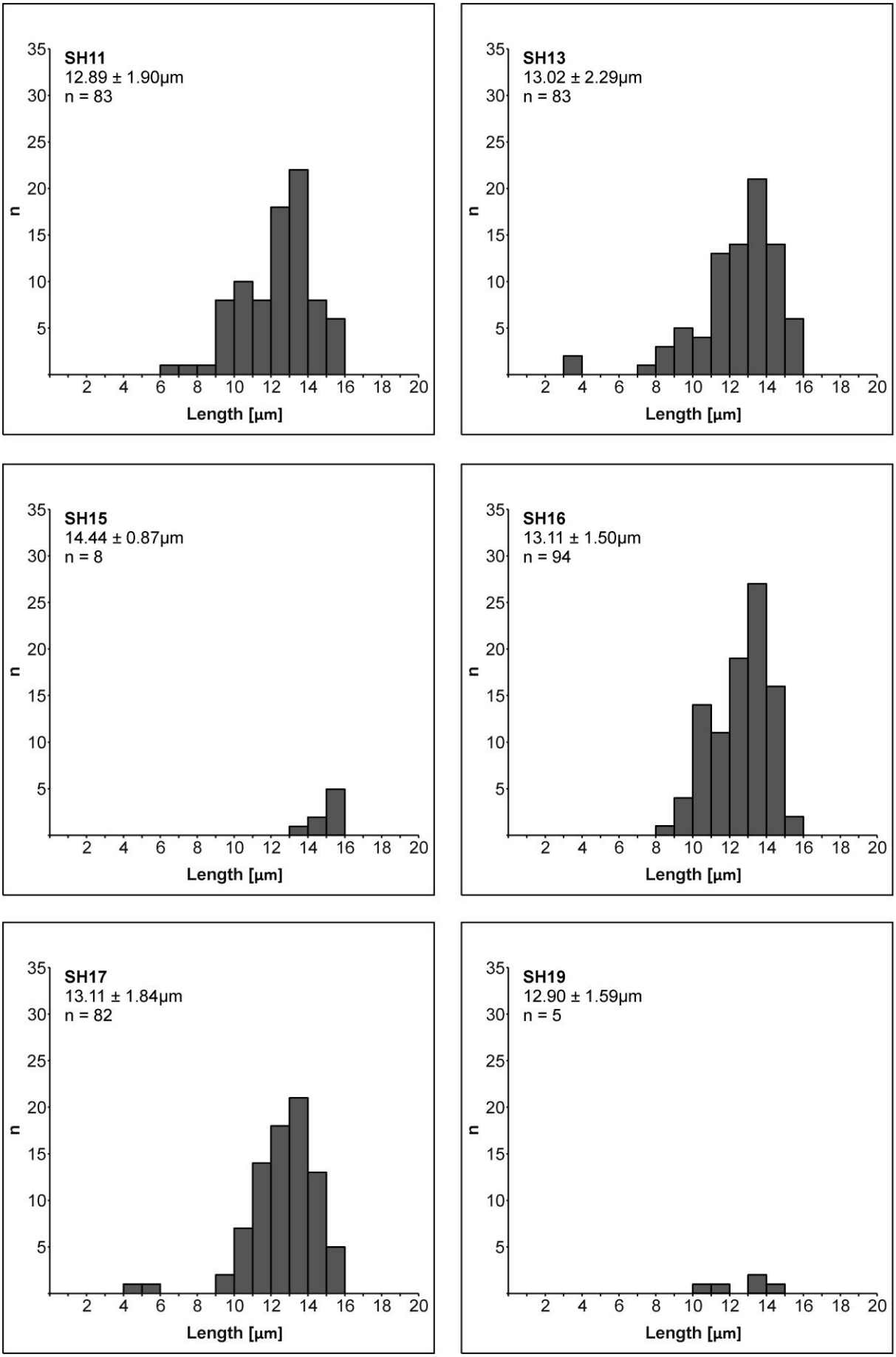

Figure S2 (continued)

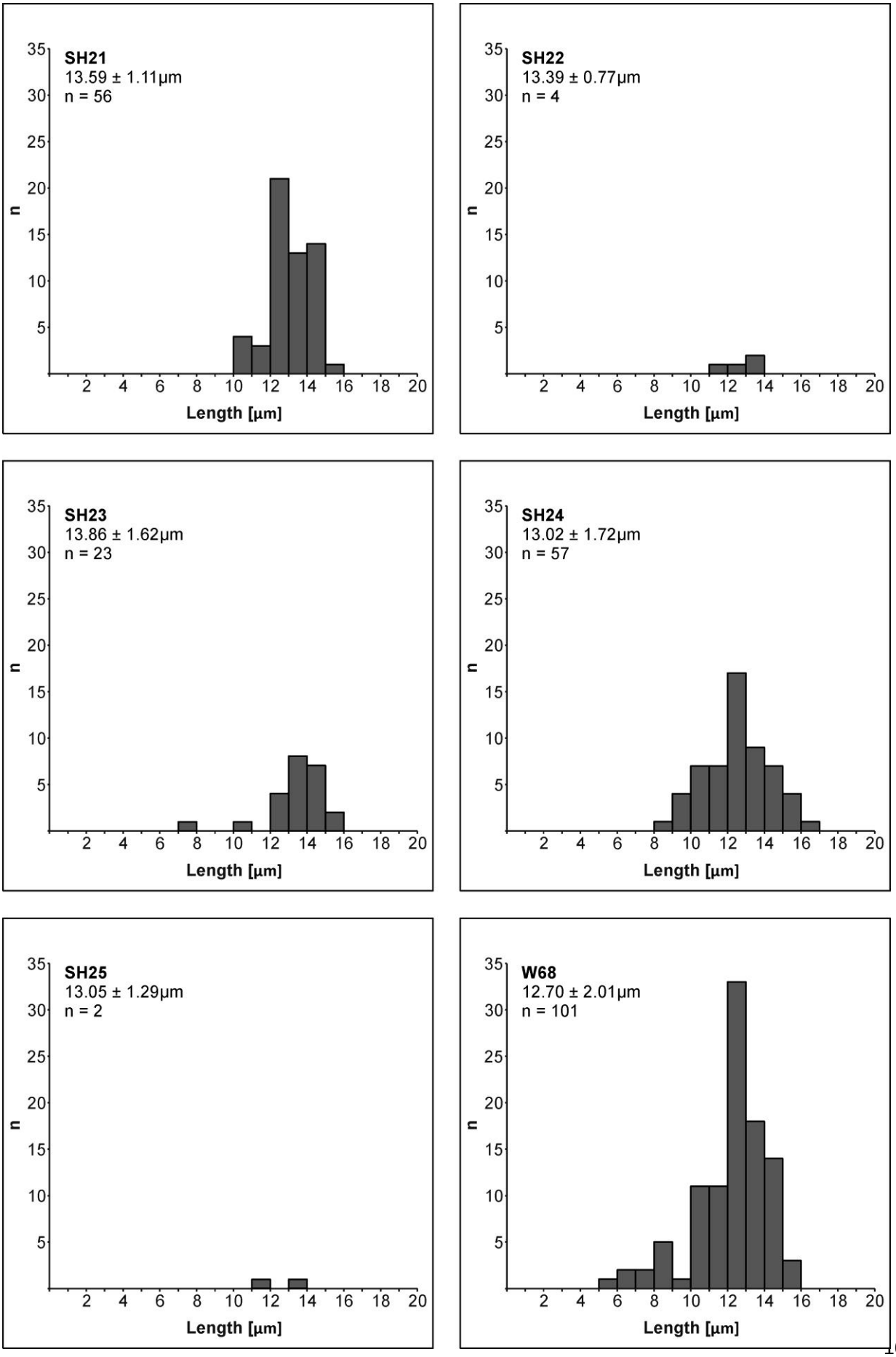

Figure S2 (continued)

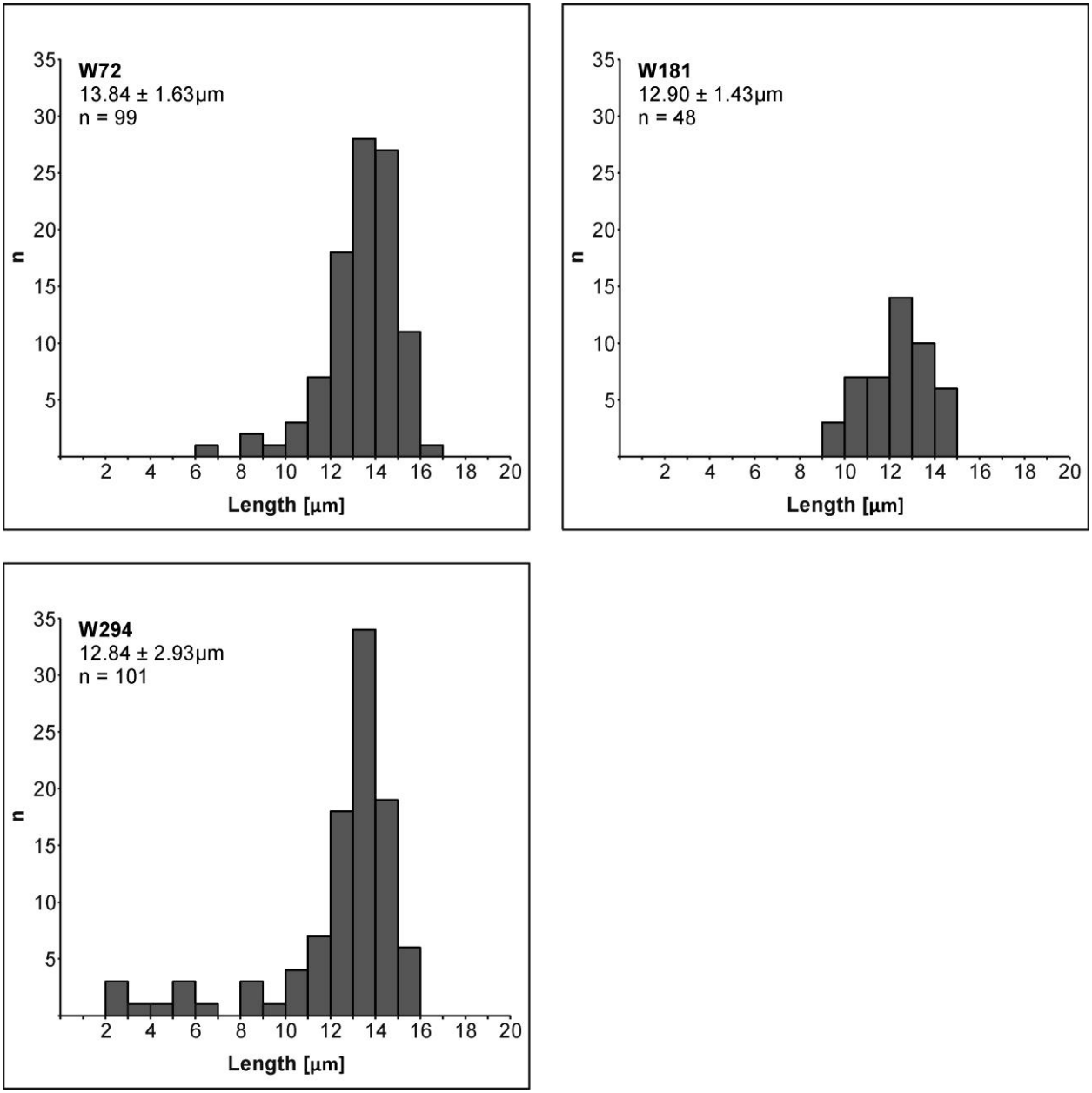

Figure S2: Track length histograms of the individual samples. Note that the lengths are not c-axis projected.

Figure S3

SH07
Arithmetic mean=214.64Ma, s.e.=27.18Ma, MSWD=13.63
Geometric mean=213.35Ma, s.e.=27.11Ma, MSWD=13.06
Central age=78.99Ma, s.e.=34.75Ma, MSWD=113.66
95% C.I=[7.93Ma, 7.93Ma]

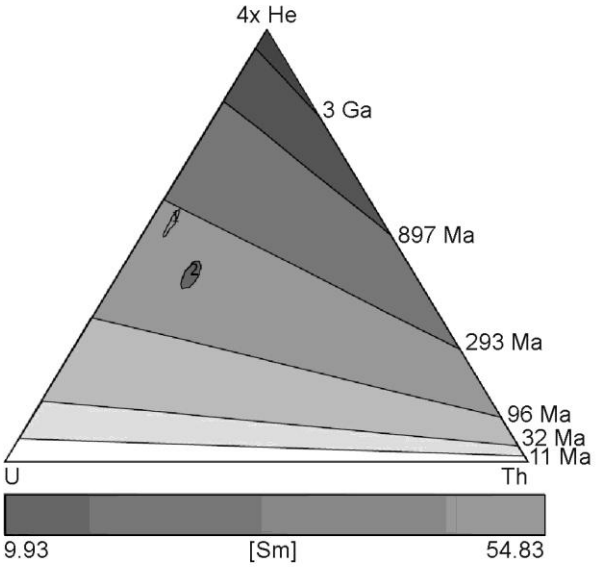

SH16
Arithmetic mean=151.00Ma, s.e.=7.29Ma, MSWD=2.28
Geometric mean=151.88Ma, s.e.=7.52Ma, MSWD=2.35
Central age=154.28Ma, s.e.=11.04Ma, MSWD=64.91
95% C.I=[132.60Ma, 170.66Ma]

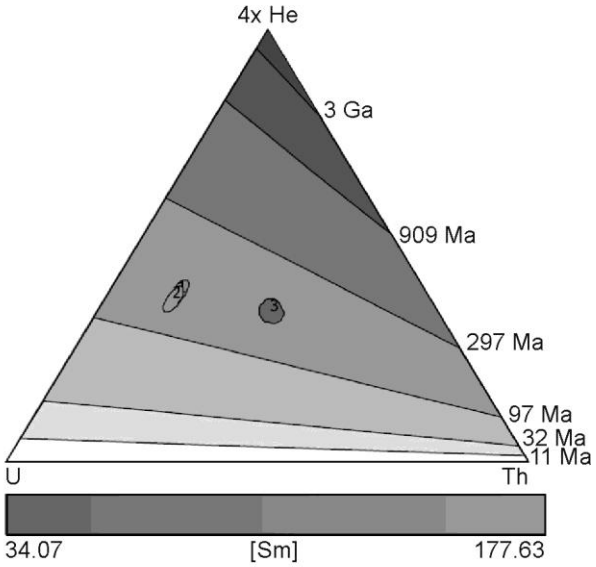

SH17
Arithmetic mean=107.86Ma, s.e.=4.24Ma, MSWD=1.89
Geometric mean=108.64Ma, s.e.=4.53Ma, MSWD=2
Central age=109.15Ma, s.e.=6.54Ga, MSWD=19.84
95% C.I=[.00ka, 808.57Ga]

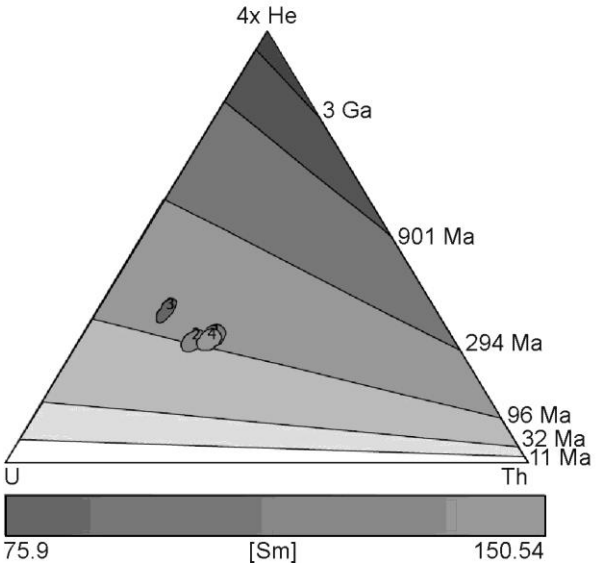

W53
Arithmetic mean=238.04Ma, s.e.=13.73Ga, MSWD=0.41
Geometric mean=237.92Ma, s.e.=13.74Ga, MSWD=0.41
Central age=245.00Ma, s.e.=12.64Ga, MSWD=509.41
95% C.I=[.00ka, 4727.24Ga]

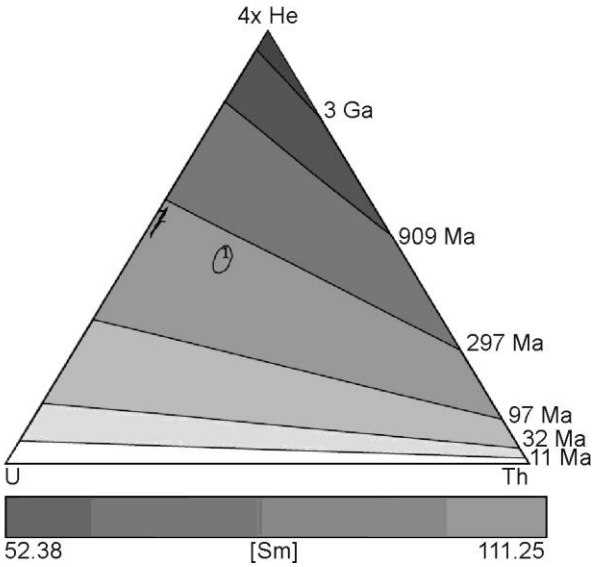

Figure S3 (continued)

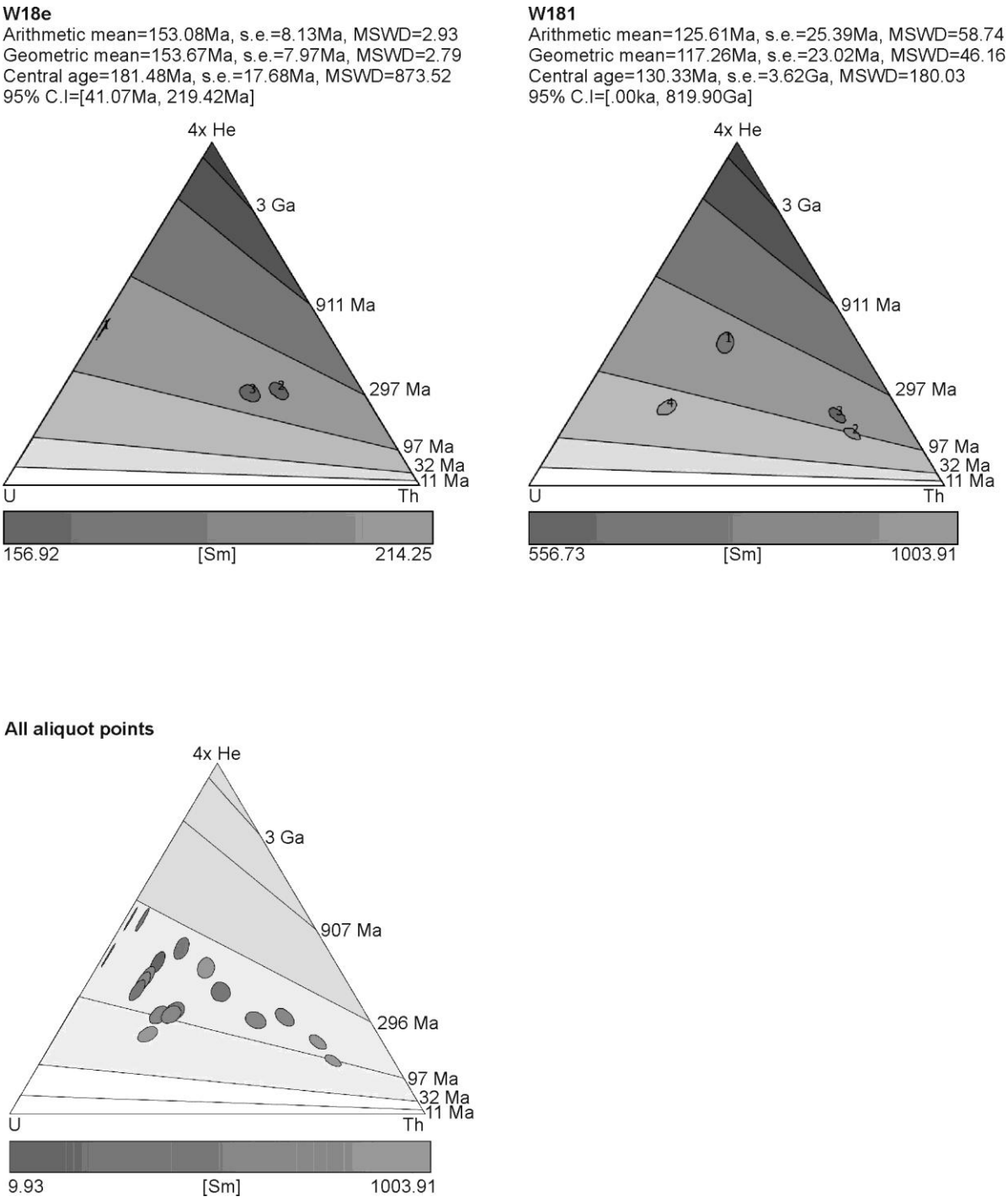

Figure S3: U-Th-He ternary diagrams and age estimations. Ellipses illustrate the 2σ error. The diagrams were created using HelioPlot (Vermeesch, 2010).

Table S4: HeFTy preferences

ZFT	AFT	AHe
Annealing Model:	Annealing model:	AHe model:
Fanning Arrhenius (Yamada *et al.*, 2007)	Ketcham *et al.* (2007)	Farley (2000) or RDAAM, Flowers *et al.* (2009)
	Initial mean track length: 16.12 ± 0.06 µm	Age α-correction: ejection
	Length reduction in standards: 0.89 µm	Stopping distance: Farley *et al.* (2011)
	c-axis projection model: Ketcham *et al.* (2007)5.0M	
	Length GOF: Kuipers Statistic	
	D_{par} Durango: 1.83 µm	
	Calibration factor: 0.9196µm	

Table illustrate the input preferences and annealing models used for thermal history modelling.

Table S5: Input constraints inverse modelling – batch mode

Constraint	$Time_{max}$	$Time_{min}$	T_{max}	T_{min}	Mode
1	300	190	320	60	2Ev
2	200	170	40	0	2Ev
3	170	1	120	-40	2Ev
4	0	0	individual surface T.		-

Table showing the input constraints used for batch mode inverse modelling. Constraints 1, 2, and 4 were set because of geological evidence, whereas constraint 3 were set widely to allow all possible iteration steps. 2Ev segment parameters were used, implying 2 times iteration between segments, with episodic and monotonic variable style. This means that cooling as well as reheating is allowed (HeFTy user guide; Ketcham (2005)).

Table S6: Individual annual mean recent surface temperatures

Sample	Lat	Lon	Elev. [m]	Mean surface temperature [°C]
SH 03	-80.422	-21.533	1110	-31±5
SH 05	-80.545	-20.767	1305	-33±5
SH 06	-80.537	-20.550	1255	-32±5
SH 07	-80.610	-20.811	1470	-35±5
SH 09	-80.545	-19.603	1335	-33±5
SH 10	-80.640	-20.625	1475	-35±5
SH 11	-80.370	-21.969	915	-29±5
SH 13	-80.455	-22.267	1105	-31±5
SH 16	-80.118	-25.633	540	-25±5
SH 17	-80.123	-25.733	720	-27±5
SH 21	-80.318	-24.983	1065	-31±5
SH 24	-80.697	-22.683	1515	-35±5
SH 25	-80.733	-23.567	1375	-34±5
W181	-80.741	-25.527	1210	-32±5
W68	-80.729	-25.003	1220	-32±5
W72	-80.695	-24.592	1250	-33±5
W294	-80.386	-30.013	570	-25±5

Table of the individual mean average surface temperature. This temperature was calculated using the mean annual temperature at sea level (ca. -18°C; Halley Station) and the orographic gradient of 0.98K/100m for dry adiabatic conditions.

Figure S4

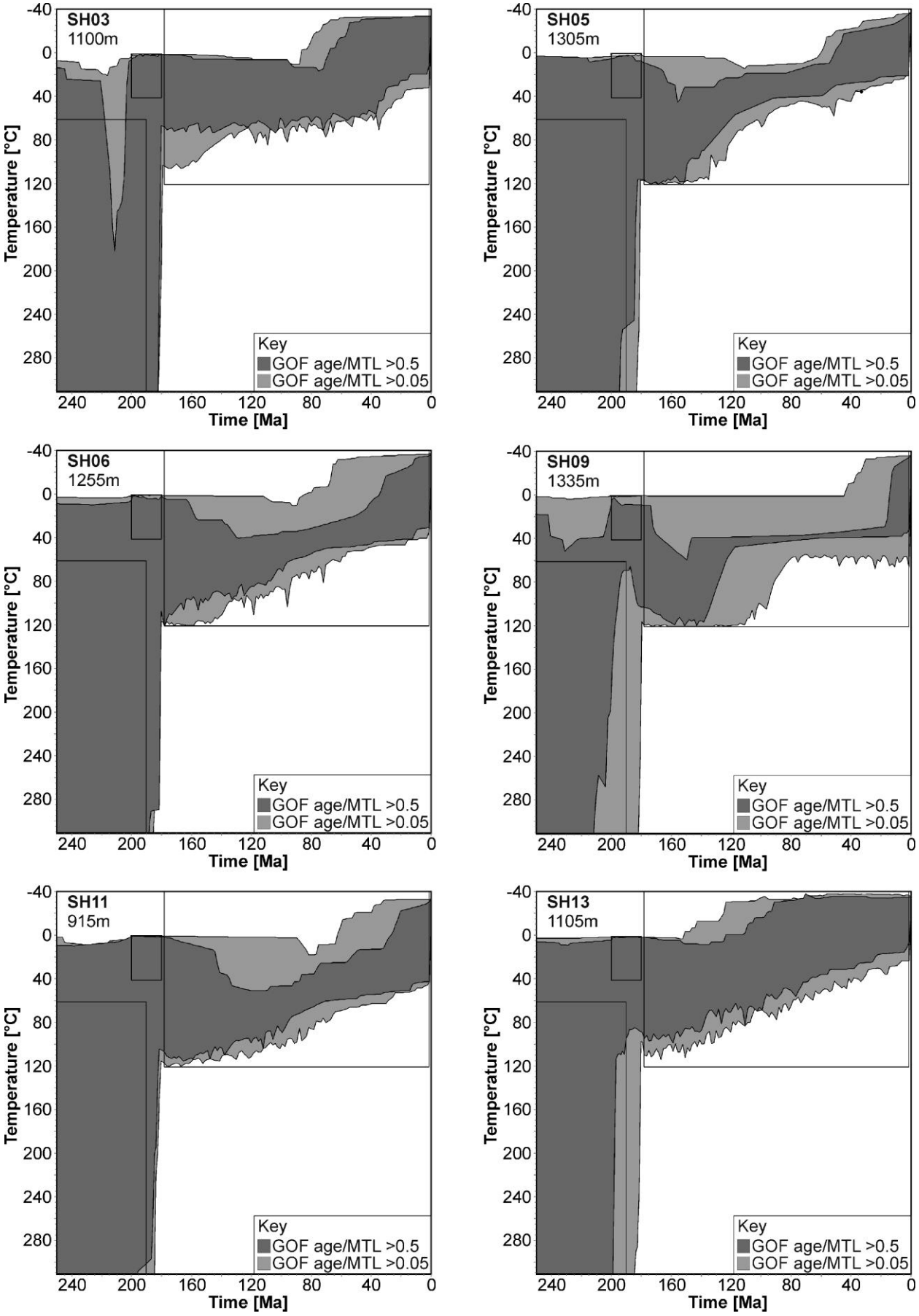
SH03
1100m
SH05
1305m
SH06
1255m
SH09
1335m
SH11
915m
SH13
1105m
Temperature [°C]
Time [Ma]
Key
GOF age/MTL >0.5
GOF age/MTL >0.05

Figure S4 (continued)

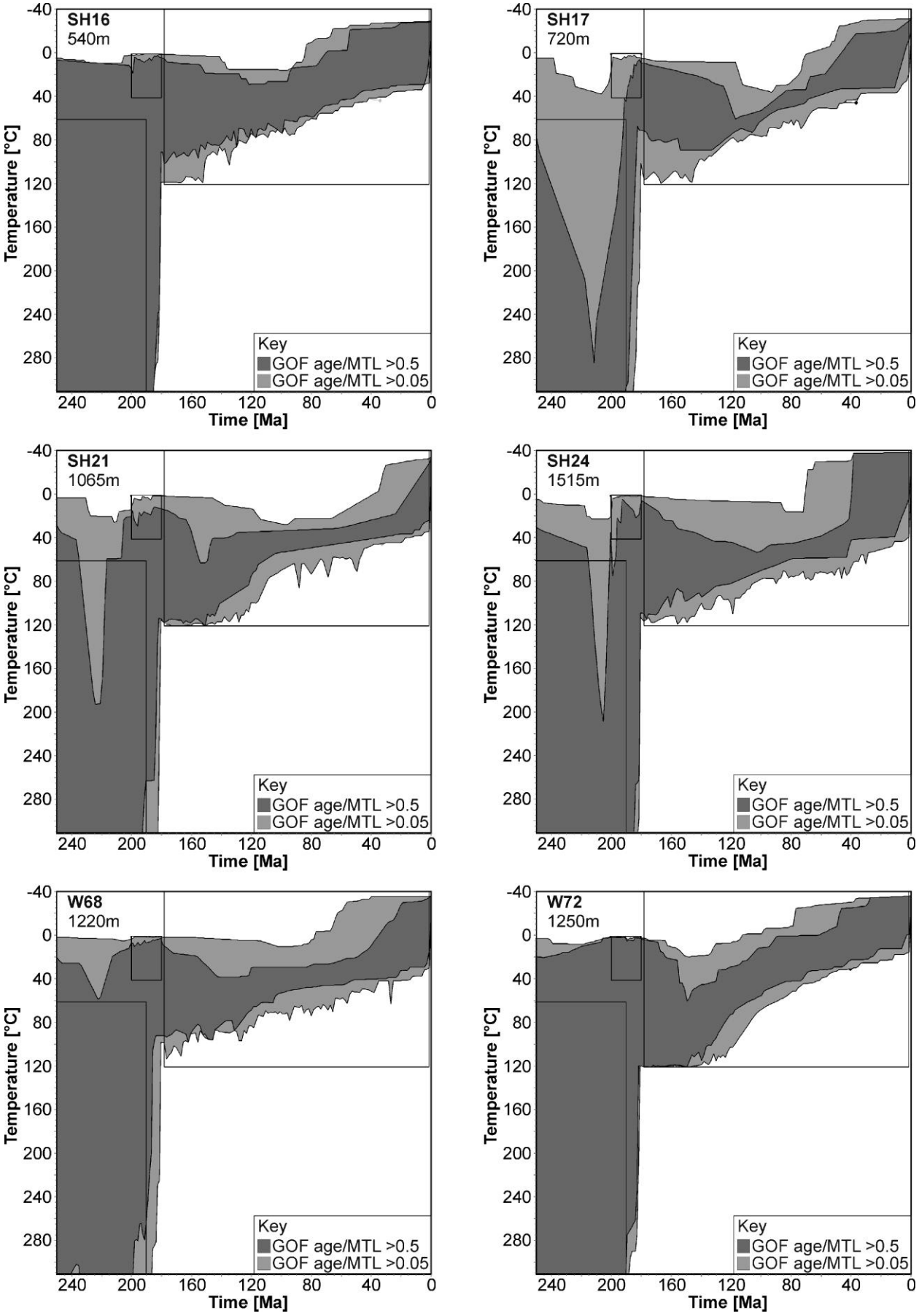

Figure S4 (continued)

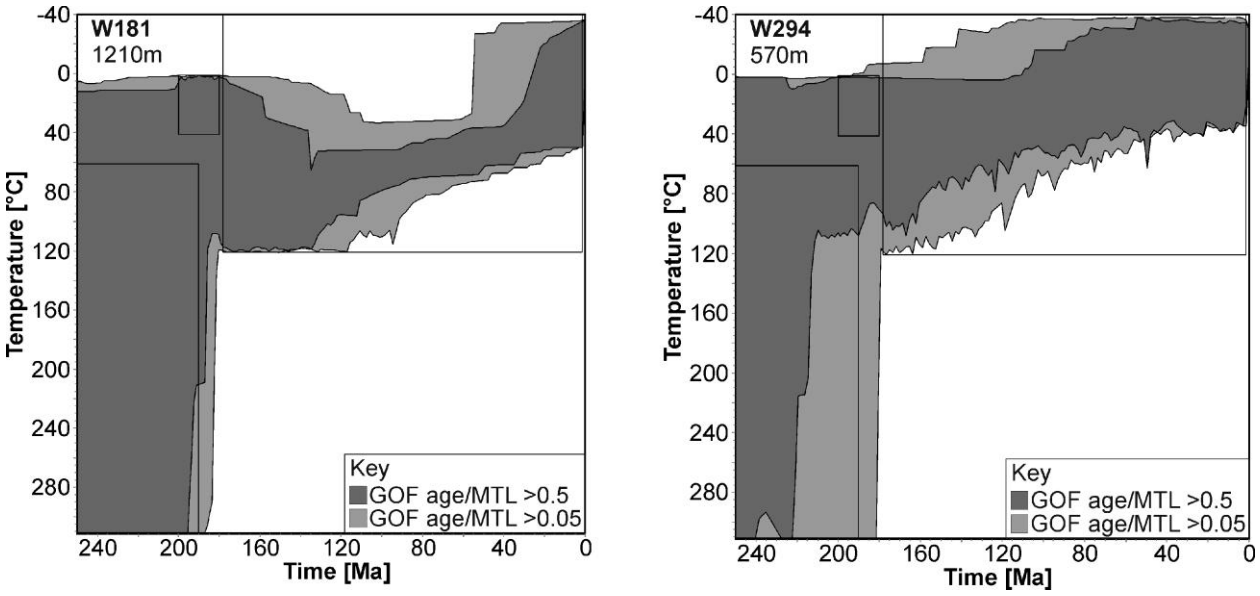

Figure S4: Inverse thermal history modelling results.

References

DE CORTE, F., VAN DEN HAUTE, P., BELLEMANS, F., INGELBRECHT, C. & NICHOLL, C. 1998. The uranium doped glass IRMM-540 distributed by the European Comission: A new tool in fission-track age calibration, 19th International Conference on Nuclear Tracks in Solids: Besancon, France.

DONELICK, R. A. 1993. Apatite etching characteristics versus chemical composition. *Nuclear Tracks Radiation Measurements* **21**, p. 604.

DONELICK, R. A., O'SULLIVAN, P. B. & KETCHAM, R. A. 2005. Apatite Fission-Track Analysis. *Reviews in Mineralogy and Geochemistry* **58**, 1, pp. 49-94.

DUMITRU, T. A. 1993. A new computer-automated microscope stage system for fission-track analysis. *Nucl. Tracks Radiat Meas.* **21**, 4, pp. 575-80.

FARLEY, K. A. 2000. Helium diffusion from apatite: General behavior as illustrated by Durango fluorapatite. *Journal of Geophysical Research* **105**, pp. 2903-14

FARLEY, K. A. 2002. (U-Th)/He dating: techniques, calibrations, and applications. *Reviews in Mineralogy and Geochemistry* **47**, 1, pp. 819-44.

FARLEY, K. A., SHUSTER, D. L. & KETCHAM, R. A. 2011. U and Th zonation in apatite observed by laser ablation ICPMS, and implications for the (U–Th)/He system. *Geochimica et Cosmochimica Acta* **75**, 16, pp. 4515-30.

FLOWERS, R. M., KETCHAM, R. A., SHUSTER, D. L. & FARLEY, K. A. 2009. Apatite (U-Th)/He thermochronometry using a radiation damage accumulation and annealing model. *Geochimica et Cosmochimica Acta* **73**, 8, pp. 2347-65.

GLEADOW, A. J. W. 1984. Fission track dating methods II - A manual of principles and techniques. In *Workshop on fission track analysis; principles and applications*, Townsville. James Cook University, p. 35.

HURFORD, A. J. & GREEN, P. F. 1982. A users' guide to fission track dating calibration. *Earth and Planetary Science Letters* **59**, 2, pp. 343-54.

HURFORD, A. J. & GREEN, P. F. 1983. The zeta age calibration of fission-track dating. *Chemical Geology* **1**, pp. 285-317.

KETCHAM, R. A. 2005. Forward and inverse modeling of low-temperature thermochronometry data. *Reviews in Mineralogy and Geochemistry* **58**, 1, pp. 275-314.

KETCHAM, R. A., CARTER, A., DONELICK, R. A., BARBARAND, J. & HURFORD, A. J. 2007. Improved modeling of fission-track annealing in apatite. *American Mineralogist* **92**, 5-6, pp. 799-810.

LASLETT, G., KENDALL, W., GLEADOW, A. & DUDDY, I. 1982. Bias in measurement of fission-track length distributions. *Nuclear Tracks and Radiation Measurements (1982)* **6**, 2-3, pp. 79-85.

SOBEL, E. R. & SEWARD, D. 2010. Influence of etching conditions on apatite fission-track etch pit diameter. *Chemical Geology* **271**, 1–2, pp. 59-69.

VERMEESCH, P. 2009. RadialPlotter: a Java application for fission track, luminescence and other radial plots. *Radiation Measurements* **44**, 4, pp. 409-10.

VERMEESCH, P. 2010. HelioPlot, and the treatment of overdispersed (U-Th-Sm)/He data. *Chemical Geology* **271**, 3-4, pp. 108-11.

YAMADA, R., MURAKAMI, M. & TAGAMI, T. 2007. Statistical modelling of annealing kinetics of fission tracks in zircon; Reassessment of laboratory experiments. *Chemical Geology* **236**, 1, pp. 75-91.